Journal of Materials Research and Technology 37 (2025) 1019–1028

Contents lists available at ScienceDirect

Journal of Materials Research and Technology

journal homepage: www.elsevier.com/locate/jmrt

Mitigating machining damage: Advanced modelling of pumice loading effects in Kevlar fibre-pumice sandwich polymer composites at the AWJM zone

Venkatesh Chenrayan [a,b], A. Saravanakumar [a], Kiran Shahapurkar [a,b,***], S. Vaishnavi [c], S. Selvam [d], Chandru Manivannan [e], Vineet Tirth [f,g], Ali Algahtani [f,h], Jana Petrů [i,*], Muhammad Nasir Bashir [i,n,o,**], Manzoore Elahi M. Soudagar [j,k], Krishna Prakash Arunachalam [l], H.M. Vidhya [m]

[a] Centre of Excellence-Advanced Materials Synthesis (CoE-AMS), Department of Mechanical Engineering, Alliance School of Applied Engineering, Alliance University, Bengaluru, 562106, India
[b] AU-Sophisticated Testing and Instrumentation Centre (AU-STIC), Alliance University, Bengaluru, 562106, India
[c] Department of Computer Science Engineering, PSG Institute of Technology and Applied Research, Coimbatore, India
[d] Department of Mechanical Engineering, Coimbatore Institute of Technology, Coimbatore, India
[e] Department of Mechanical Engineering, Dhirajlal Gandhi College of Technology, Salem, 63840: India
[f] Mechanical Engineering Department, College of Engineering, King Khalid University, Abha, 61421, Asir, Kingdom of Saudi Arabia
[g] Centre for Engineering and Technology Innovations, King Khalid University, Abha, 61421, Asir, Kingdom of Saudi Arabia
[h] Research Center for Advanced Materials Science (RCAMS), King Khalid University, Guraiger, PO Box 9004, Abha, 61413, Asir, Kingdom of Saudi Arabia
[i] Department of Machining, Assembly and Engineering Metrology, Faculty of Mechanical Engi-neering, VŠB Technical University of Ostrava, Ostrava, Czech Republic
[j] Centre for Research Impact and Outcome, Chitkara University Institute of Engineering and Technology, Chitkara University, Rajpura, 140401, Punjab, India
[k] Centre for Promotion of Research, Graphic Era (Deemed to be University), Clement town, Dehradun, India
[l] Departamento de Ciencias de la Construcción, Facultad de Ciencias de la Construcción Ordenamiento Territorial, Universidad Tecnológica Metropolitana, Santiago, Chile
[m] Centre of Molecular Medicine and Diagnostics (COMManD), Saveetha Dental College and Hospitals, Saveetha Institute of Medical and Technical Sciences, Saveetha University, Chennai, 600 077, India
[n] Department of Mechanical Engineering, University of Malaya, 50603, Kuala Lumpur, Malaysia
[o] Multi-Scale Fluid Dynamics Lab, Department of Mechanical Engineering, Yonsei University, Seoul, 120-749, Republic of Korea

ARTICLE INFO

Handling editor: SN Monteiro

Keywords:
Kevlar fibre
Pumice
Delamination
Kerf taper
Surface roughness
Grey relational analysis (GRA)
Machine learning (ML)

ABSTRACT

The development of varieties of fibre-reinforced polymer composite (FRP) has become a part of day-to-day life and is the core agenda of the manufacturing industries in new product development. Despite the wider applications, the machining of FRPs is encountering a greater challenge in overcoming the machining damage. It is the right proposal to deplete the prominent machining damages like kerf taper, delamination and surface roughness by introducing novel hybrid statistical and soft computing models. The novel Kevlar fiber woven mat-pumice particles reinforced sandwich is fabricated using open moulding and machined with Abrasive Water Jet Machining by following L9 orthogonal guidelines. The three different pumice compositions, standoff distance, abrasive flow rate and hydraulic pressure were considered the prime variables to influence the damages. The hybrid analysis results declare that trial No.3 is an optimal parameter, which comprises 100 (MPa) of hydraulic pressure, 2 mm of standoff distance, 300 (gm/min) of abrasive flow rate and 10 % of pumice particles to scale

* Corresponding author.
** Corresponding author. Department of Machining, Assembly and Engineering Metrology, Faculty of Mechanical Engi-neering, VŠB Technical University of Ostrava, Ostrava, Czech Republic.
*** Corresponding author. Centre of Excellence-Advanced Materials Synthesis (CoE-AMS), Department of Mechanical Engineering, Alliance School of Applied Engineering, Alliance University, Bengaluru, 562106, India.
E-mail addresses: venkyachvsh@yahoo.co.in (V. Chenrayan), skumar3011@gmail.com (A. Saravanakumar), kiranhs1588@gmail.com (K. Shahapurkar), vaishnavi1731@gmail.com (S. Vaishnavi), selvams2901@gmail.com (S. Selvam), mechchandru123@gmail.com (C. Manivannan), vtirth@kku.edu.sa (V. Tirth), alialgahtani@kku.edu.sa (A. Algahtani), jana.petru@vsb.cz (J. Petrů), m.nsr8080@yahoo.com (M.N. Bashir), me.soudagar@gmail.com (M.E.M. Soudagar), k.prakash@utem.cl (K.P. Arunachalam), hm.vidyakiran@gmail.com (H.M. Vidhya).

https://doi.org/10.1016/j.jmrt.2025.06.007
Received 15 April 2025; Received in revised form 14 May 2025; Accepted 1 June 2025
Available online 3 June 2025

down the damages. A noticeable 1.69 %, 25.12 % and 40.71 % decrement in machining damages, along with the finding of a higher contribution of pumice content in minimizing the damages, would benefit the FRP industries to march towards the implementation of lean manufacturing and new product development (NPD).

1. Introduction

The fibre-reinforced polymer composite is a divine angel born between natural and synthetic fibres. This novel material remarkably contributed to replacing the existing monolithic materials in almost all sectors. In particular, the synthetic fibre-reinforced composites are completely diffused in all product-based areas associated with the industrial and social community [1–3]. They are being used more and more in the biomedical [4], mechanical [5], aerospace [6], transportation [7], marine [8], and construction [9] sectors due to their reduced environmental impact, low energy consumption, and corrosion resistance. There are umpteen research outcomes [10–12] dealing with synthetic fibres carbon, glass, Kevlar, basalt, polyester and nylon fibre monotonically or hybrid reinforced with different particles Al_2O_3, B_4C, SiC, ZrO_2, TiB_2, TiC, TiO_2, nano clay, cenosphere, eggshell, wood flour, and Hallow Glass Micro Balloons (HGMB). Apart from these, synthetic fibre woven sandwich composites cored with particulate [13] or lattice structures [14] have also impacted product development in terms of increased product life cycle. The outcomes are highly deliverable to lay a greater road to increase the performance of the product by reducing the weight. However, the non-homogeneity in the structure and the involvement of high-strength fibres pose a great challenge in the machining of these composites [15]. The inevitable machining damages like delamination, fibre pull-out, and matrix cracking in quantified magnitude were reported with conventional machining methods [16]. Indeed, Abrasive Water Jet Machining (AWJM) is a proven and flexible unconventional machining method to fabricate these composites. Unfortunately, the kerf taper on the thickness of the walls supplemented by the loss of kinetic energy between the top and bottom layer is a prominent menace in the AWJM process [17]. The usual delamination and surface roughness are also the machining damages which dent the machining quality. This research study advocates the inclusion of pumice particles in the core of the Kevlar fibre woven sandwich composite. It is expected to enhance the bonding strength of the cover sheets with the core through the poorer surface nature of the pumice particles. Pumice stone is a naturally occurring volcanic glassy rock that is primarily composed of silicon dioxide (SiO_2) [18]. Induced pumice occurs when the magma cools suddenly and the internal gases lose pressure. The dissolved gases that precipitate during cooling as lava screams across the atmospheric air give pumice its porous structure [19]. However, the potential nature of the pumice particles in mitigating the delamination effect of the Kevlar fibre woven pumice sandwich composite, along with other machining damages, surface roughness and kerf taper during the machining at AWJM is of prominent interest. Moreover, these machining damages are not only a primary cause of the material but also driven by the machining parameters and their levels [20]. Hence, the intervention of deeper science is required to machine this fibre-reinforced composite with minimal damage. Coping with this, many researchers attempted to implement various statistical tools Principal Component Analysis (PCA) [21], Grey Relational Analysis (GRA) [22], Taguchi's experiment design [23] and Response Surface Methodology (RSM) [24] to minimize the machining damages in the AWJM zone by involving different variants of fibres, particles and weaving structure. In addition to that, the advanced prediction techniques Ant Colony Optimization (ACO) [25], Genetic Algorithm (GA) [26], Particle Swarm Optimization (PSO) [27], Simulated Annealing (SA) [28], and Technique for Order Preference by Similarity to Ideal Solution (TOPSIS) [29] are also used to enhance the machining qualities by the various researchers. The emerging technologies of Machine Learning and Artificial Intelligence (AI) are also helpful in predicting the optimal combination of variables, along with the reinforcement to scale down the machining damages.

The main goal of this research is to reduce major machining damages like delamination, kerf taper, and surface roughness to improve the machining quality of waste material-reinforced polymer sandwich composites. Further, the recycling of waste material under the arena of waste to wealth and the subsequent ease are also extended objectives. The substitution for existing monolithic material, engaged in structural and constructional applications by Ethiopian pumice particle embedded in the epoxy core and covered by the resin-impregnated Kevlar fibre woven sandwich composite, is regarded as the prime novelty of the study. Authors affirm that none of the work reported emulates Kevlar fibre woven cover sheet-pumice loaded core, epoxy sandwich panels. Further, the deployment of hybrid GRA integrated ML techniques, Linear regression and Shapley Additive Explanation (SHAP) to downsize the magnitude of AWJM's machining menaces, delamination, kerf taper, and surface roughness represents a significant advancement in the novelty. Apart from including pumice, the approach of fabricating the sandwich composite with a particulate-filled core, to address the structural application is distinctive and enhances its originality. Based on a critical literature survey and the author's knowledge, machining damage minimization of Kevlar-woven pumice-reinforced sandwich panels through hybrid GRA-ML (Linear regression, SHAP) has never been narrated.

2. Materials and methods

2.1. Preparation of sandwich composite

Solind Services Private Limited in Bengaluru was chosen to purchase 500 g of K6 Hardener and 3 kg of L12 epoxy (Lapox). A 1 × 1 m piece of Kevlar woven fabric (PT003) was purchased from Gogreen Products in Chennai. Table 1 Displays the technical details of Kevlar woven fabric. Pumice stones collected from Awash National Park, close to the Ethiopian capital of Adama, are depicted in Fig. 1(a). The collected stones were heated to 150 °C outdoors to release insects and worms. As confirmed by the particle analyzer results displayed in Fig. 1(b), the preheated pumice stones were reduced to 30 μm, and the size was managed using a 30 μm sieve.

The composite sandwich panel made using the open moulding technique and its cross-section are depicted in Fig. 2, along with the schematic arrangement of the sandwich. Fig. 3(a) shows the wax-applied die that was used to cast the composite samples. The Kevlar mat is primarily sized to fit inside the die at 100 mm × 100 mm. Acetone was used to clean the Kevlar woven fabric mat of dirt and foreign contaminants. Wax is applied to the bottom die plate surface to facilitate the casted composite's core easy removal from the die. As seen in Fig. 3 (b) resin resin-impregnated cover sheets were prepared for both sides of the sandwich. A measured quantity of epoxy resin to accommodate a 4 mm core thickness was mixed with a predetermined quantity of pumice particles in a beaker. There were four different variants of sandwich core comprising the pumice weight percentages of 5, 7.5 and 10. Then, Sonification was done for 40 min to make sure the resin and Pumice particles were mixed uniformly. Since the strength of the sandwich

Table 1
Technical details of Kevlar mat [30].

Grade	Weight (g/m2)	Weaving style	Thickness (mm)
PTOO3	200	Twill	0.26

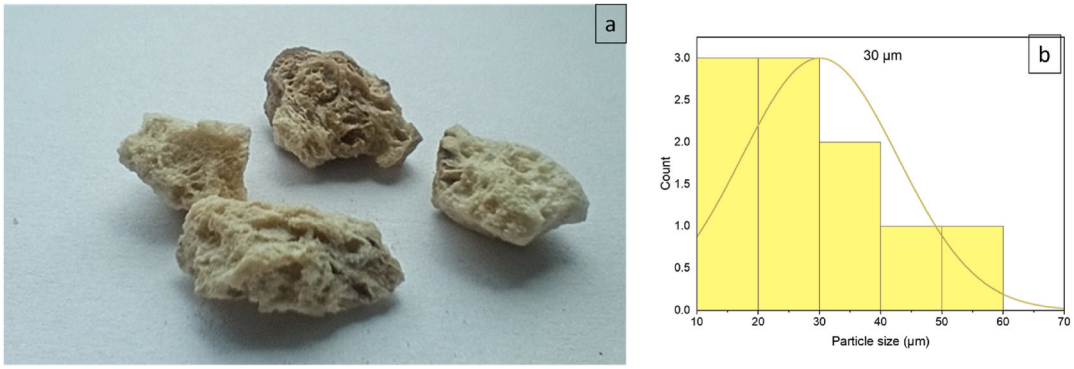

Fig. 1. (a) Pumice stone (b) Particle size analysis result.

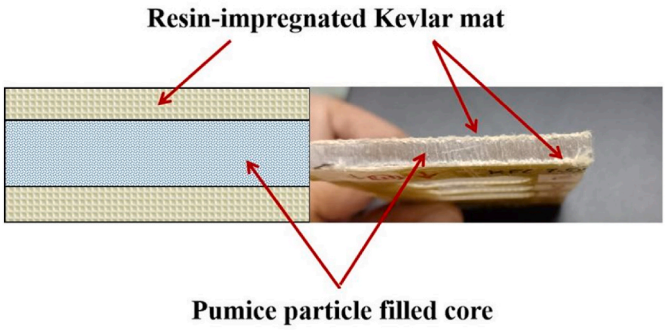

Fig. 2. Schematic arrangement of the cross-section of Kevlar-Pumice particle-filled sandwich.

composite relies on the interfacial bonding between the core and cover sheets, both sides of the surfaces of the cores were made rougher before the placement of the cover sheet. A mat of resin-impregnated Kevlar woven fabric was positioned on the die's bottom side. A glass rod was used to evenly distribute Pumice particles and resin onto a Kevlar woven fabric mat that is stored on the die's bottom side. Another resin-impregnated Kevlar mat was placed over the die after it had been poured and filled. Additionally, to guarantee a better setting of the composite, an airtight compression process was performed before curing the sandwich.

2.2. AWJ machining and experimental procedure

The laminates made of composite were machined using a Computer Numerical Controlled abrasive water Jet Cut 16F-31 supplied by "An Innovative International Limited.", as indicated in Fig. 4 (a) A rigid cantilever serves as the main structural component of the machine, which has dimensions of 5500 mm in length, 2754 mm in width, and 2250 mm in height overall. Up to 600 kg/m^3 of load can be supported by the machine. Additionally included elements are Schneider digital AC servo motors with incremental encoders. The linear and non-linear flow rates of its abrasive metering system range from 0 to 1000 g/min. The abrasive Water Jet cutting head is composed of three parts: (i) a 0.28 mm nozzle aperture that creates a stream of water jet that is collimated from high-pressure water; (ii) an abrasive mixing chamber that uses the venturi effect to combine abrasive particles with the water jet; and (iii) a focusing head that is diameter of 0.8 mm and length 76 mm. As abrasive particles, an 80-mesh AG garnet was used. Compressed air was used to transfer the abrasive mass from a hopper to the focusing head, and the flow rate was controlled by a vision control system.

Nine experimental trials were carried out by monitoring the machining parameters at three distinct levels following Taguchi's robust design. The standoff distance, feed rate, water pressure, and abrasive flow rate were the machining parameters taken into account. After closely examining previous studies, the machining parameters and their corresponding levels are arrived at as shown in Table 2. The three main machining damages, kerf taper, delamination and surface roughness, are the basis for the responses. Kerf width detects the incorrect width distribution on the slot's upper and lower sides. The kerf ratio can also be used to determine the degree of width irregularity. Another common damage that happens to FRP when it is machined using AWJM is delamination.

2.3. Measurement of responses

Using a Celestron Capture Pro stereo microscope built with Micro Capture Pro software interface, the hybrid FRP specimen's bottom and

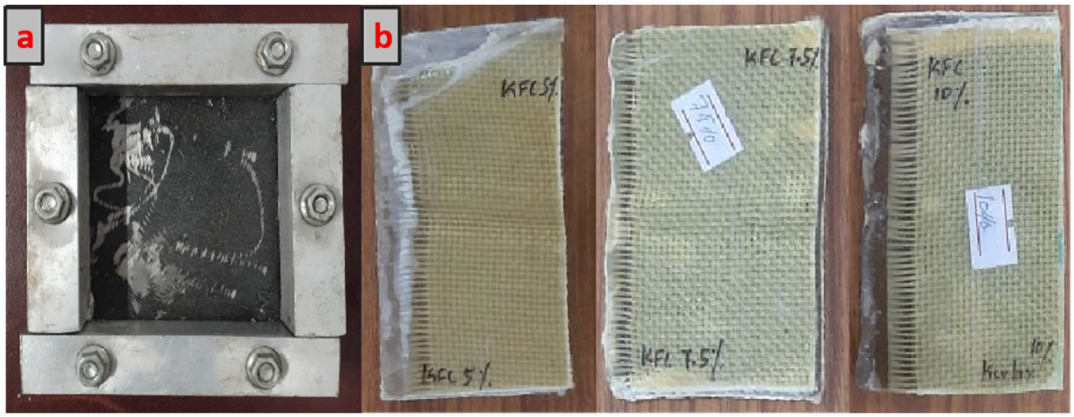

Fig. 3. Processing of sandwich composite (a) Die used (b) Processed sandwich composites.

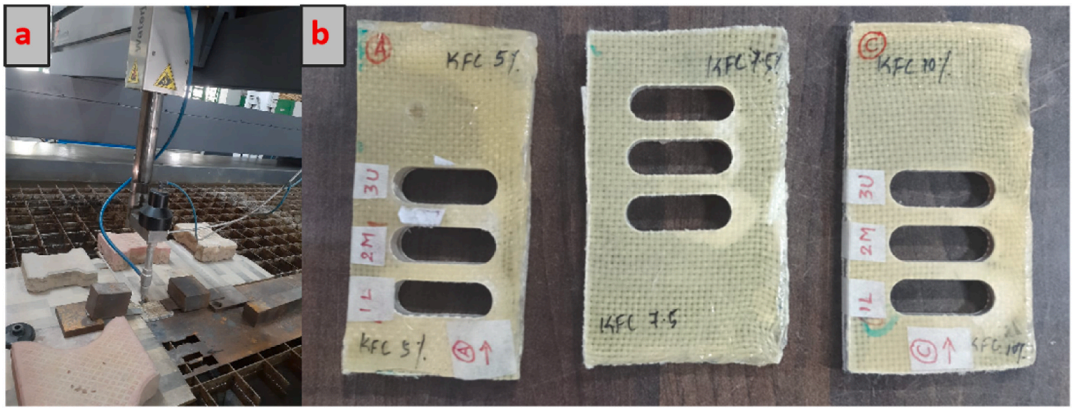

Fig. 4. (a) AWJM (b) Machined specimen of Kevlar-Pumice particle-filled panels.

Table 2
Machining parameters and their levels [21].

Parameters	Level 1	Level 2	Level 3
Standoff Distance (mm)	2	3	4
Hydraulic Pressure (MPa)	80	90	100
Abrasive flow rate (g/min)	200	250	300
Pumice Composition (wt.%)	5	7.5	10

top kerf widths were measured to generate output data. Three readings were taken along the edges from three different locations, and the analysis considered the average value into account. Delamination occurs when the integrity between the layers is compromised during the processing of layered materials. The Micro Capture Pro software vision measurement system is used to analyse the characteristics of the delaminated surface. To capture and store high-resolution specimen images and videos, the machined specimen edges were held up to the digital 5mp high-resolution sensor and parallel to the granite table. Three pictures were captured at three different locations along the edge for each delamination thickness, and the average value was then utilized for modelling. The Surftest SJ210 series was used to measure the surface roughness at three various locations on the machined surface, and the mean of these values is taken into account for the analysis.

2.4. Design of experiments

To minimize the resources involved in the machining, Taguchi's robust design was implemented. Nine experiments were carried out using the L9 orthogonal array, which was selected based on the specified machining parameters and their levels. Table 3 lists the combinations of the recorded responses and the machining parameters.

3. Statistical approach

3.1. Grey Relational Analysis (GRA)

Statistical modelling is typically used to determine the best parameters to achieve the goals in the desired performance characteristics. Specifically, a few modelling approaches are available to address multi-objective problems. One of the multi-objective statistical modelling tools is Grey Relational Analysis (GRA), in which the multi-objectives are converted into a single unitless quantity known as Grey Relation Grade (GRG) [21,31]. The minimization of variance through the involvement of normalization of signal-to-ratio (S/N) and representing them between 0 and 1 is also a unique feature of GRA. Meanwhile, the S/N ratio is fixed according to the nature of the performance characteristics of the responses. However, the responses are all machining damages, which should be minimized as much as possible. [32]; hence, the lower the better scenario of the S/N ratio [33], as shown in Fig. 5 was employed. Based on the equations depicted in the GRA functional chart, the normalised S/N ratios, Grey Relational Coefficients (GRC) values, and Grey Relational Grade values are computed and the same are furnished in Table 4.

4. Soft computing approach

Nowadays, Machine Learning has revolutionised most of fields through its capability to solve complex problems. In advanced manufacturing processes, it provides the ability to find non-linear relationships that are complex to address conventionally. It offers a framework to identify, quantify and find feature significance in complex machining processes. Unlike statistical analysis, which handles linearity in data, machine learning algorithms find the dependencies and interactions in the data. [35]. In the advanced AWJM process of Kevlar Pumice composite, it is essential to identify the relationships between the features such as pumice composition, hydraulic pressure, SOD and abrasive flow rate. The key responses are machining damages like Kerf

Table 3
Experimental observation of machining damages.

Exp No	Standoff Distance (mm)	Hydraulic Pressure (bar)	Abrasive Flow rate (g/min)	Pumice Composition	Kerf ratio (Length)	Kerf Ratio (Width)	Delamination (mm)	Surface roughness (μm)
1	2	80	200	5	1.012	1.017	0.257	2.2138
2	2	90	250	7.5	1.0055	1.013	0.2003	2.745
3	2	100	300	10	1.005	1.002	0.15895	2.456
4	3	80	250	10	1.006	1.032	0.2009	3.344
5	3	90	300	5	1.0095	1.027	0.2302	2.926
6	3	100	200	7.5	1.0058	1.024	0.2201	3.056
7	4	80	300	7.5	1.0065	1.0185	0.2123	4.122
8	4	90	200	10	1.009	1.017	0.2429	3.321
9	4	100	250	5	1.007	1.021	0.2035	3.762

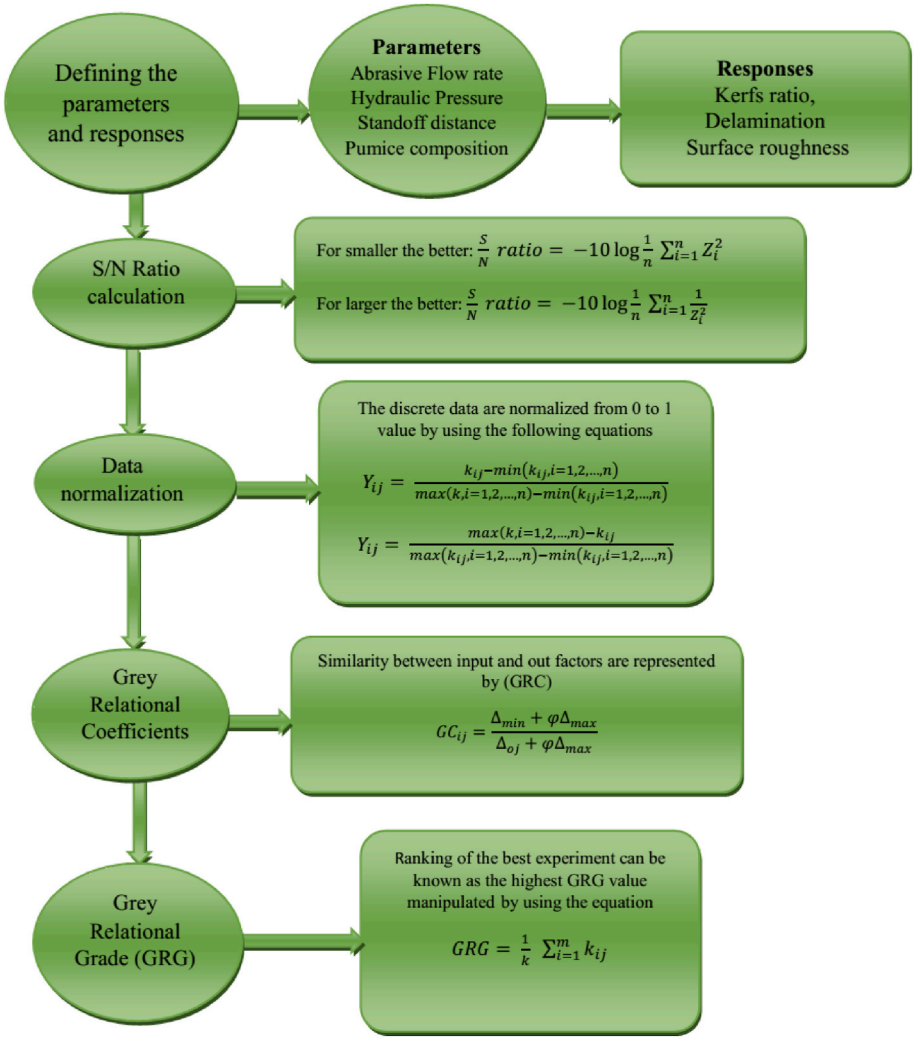

Fig. 5. Functional chart for GRA [34].

Table 4
Computed grey relational coefficients (GRC) and grades (GRG).

Signal-to-Noise Ratio				Grey Relational Coefficients				Grey Relational Grade (GRG)
Kerf ratio (Length)	Kerf Ratio (Width)	Delamination (mm)	Surface roughness	Kerf ratio (Length)	Kerf Ratio (Width)	Delamination (mm)	Surface roughness	
−0.1036	−0.1464	11.8013	−6.9028	0.3333	0.5000	0.3333	1.0000	0.5417
−0.0476	−0.1122	13.9664	−8.7708	0.8750	0.5769	0.5425	0.6424	0.6592
−0.0433	−0.0174	15.9748	−7.8046	1.0000	1.0000	1.0000	0.7975	0.9494
−0.052	−0.2736	13.9404	−10.485	0.7778	0.3333	0.5389	0.4578	0.5269
−0.0821	−0.2314	12.7579	−9.3255	0.4375	0.3750	0.4076	0.5726	0.4482
−0.0502	−0.206	13.1476	−9.7031	0.8140	0.4054	0.4450	0.5311	0.5489
−0.0563	−0.1592	13.461	−12.302	0.7000	0.4762	0.4789	0.3333	0.4971
−0.0778	−0.1464	12.2914	−10.425	0.4667	0.5000	0.3687	0.4629	0.4496
−0.0606	−0.1805	13.8287	−11.508	0.6364	0.4412	0.5239	0.3813	0.4957

Ratio (Length and Width), delamination and roughness. [36]. To predict the significant set of parameters, including pumice composition to downsize the machining damages, two predictive modelling techniques, namely Linear Regression and SHAP (Shapley Additive Explanations), were employed.

4.1. Linear regression

The significance of AWJM parameters along with the pumice composition was evaluated using Linear Regression, which employed the T-values for predicting the ranking significance as shown in Fig. 1. Linear Regressions provide a basic understanding of feature significance by using regression coefficients, t-values and p-values. In this study, T-value is used for assessing feature significance as it provides both magnitude and sign of T-values in turn indicating the strength and direction of influence of the features on the dependent variable. Raw coefficients are prone to problems in feature scaling, P-values offer binary significance, but T-values provide a ranked measure of each feature's relative importance. Based on the analysis, pumice composition exhibits a higher significance, confirming its dominance over the machining

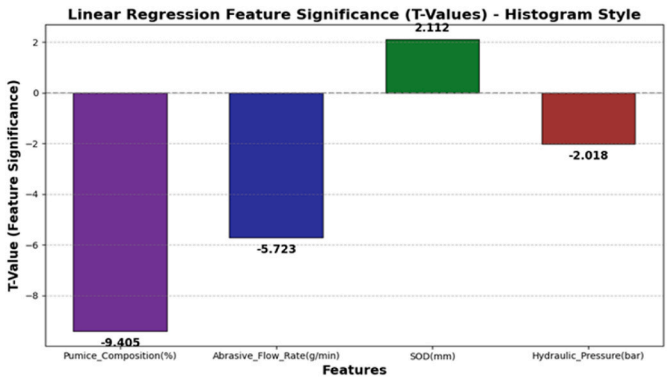

Fig. 6. Significance of parameters predicted by linear regression.

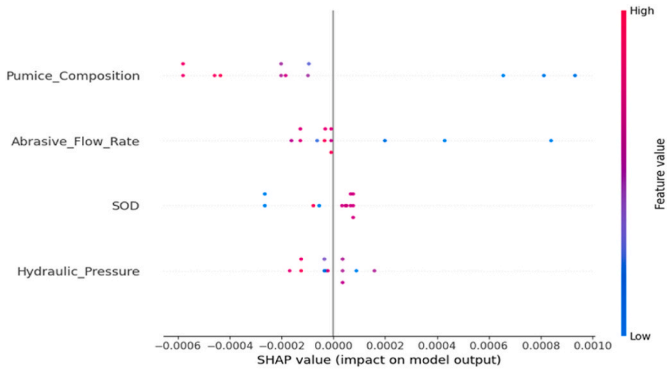

Fig. 7. Significance of parameters predicted by SHAP.

damages. Next, the abrasive flow rate with a T-Value of −5.723 shows it is the second most significant one, highlighting its importance in the machining responses. SOD and Hydraulic Pressure hold as the third and fourth features important for prediction respectively. Negative T-Values show an inverse relationship between feature and machining response. SOD has a positive effect while Hydraulic pressure shows a moderate effect. The t-value can be computed by using the following equation.

$$t\ value = \frac{\beta i}{SE(\beta i)} \tag{1}$$

where t value represents the T-Value, βi represents the regression coefficient, and SE is the standard error of βi.

4.2. Shapely additive explanations (SHAP)

SHAP, on the other hand, represents a state-of-the-art machine learning technique that assigns Shapley value to each feature, measuring contribution to prediction. It demonstrates the ranking significance of the parameters on the responses considered. In this study, SHAP was employed to interpret the significance order of the features used in AWJ machining of Kevlar-pumice sandwich composites. SHAP is prone to provide visual and data-driven explanations of feature contribution. The SHAP plot shown in Fig. 2 reveals that pumice composition has widespread SHAP values, showing it has a greater influence on the machining damages considered. The abrasive flow rate shows a similar pattern but is less dense than the pumice composition. The third feature is, SOD has secured lesser SHAP values than both pumice composition and abrasive flow rate, hence its significance is not appreciated. Hydraulic pressure is the least significant because of its poorer SHAP values.

The influence of feature parameters using both linear regression and SHAP allows for both statistical significance testing and model interpretability. The linear regression model showed an R^2 value of 0.76, indicating the model's ability to validate the results. Statistical significance was confirmed through an F-test ($F = 19.46$, $p < 0.001$. The model is also validated by performing 5-fold cross-validation, and the residuals were examined. The Durbin-Watson statistic indicated the absence of autocorrelation, while the Jarque-Bera test reflected mild non-normality in residuals, which is common in experimental machining studies. Fig. 6 shows the visual impact of features in prediction using t-values. The SHAP plot in Fig. 7 shows the summary of contributions of features. SHAP could capture interaction effects and local patterns not modelled linearly. Through the integration of regression-based statistics and SHAP values, a more comprehensive understanding of features was obtained. This combination allowed interpretation of model behaviour both globally and locally, thereby improving conclusions and reducing overfitting.

The optimal machining parameters, including the pumice composition, need to be identified, which is time-consuming in traditional methods but done effectively using AI & ML algorithms [36]. In this study, the Genetic Algorithm is used as an optimization technique to find global optimal solutions. It offers a bio-inspired, robust and efficient optimization algorithm for exploring complex solution spaces. They use the principles of natural selection to operate on a potential population with selection, crossover, fitness evaluation and mutation steps. A Random Forest regression model was first trained on the experimental data to predict responses. The Genetic Algorithm was then applied to this predictive model to search for better parameters. The algorithm derived the combination of SOD = 2 mm, Hydraulic Pressure = 100 bar, Abrasive Flow rate = 300 g/min and Pumice Composition of 10 % as an optimal one. The algorithm identified these values with the combined score of 4.6219, closely matching experiment no 3 in the dataset, thereby validating trial No.3 as the ideal experiment. A comparative bar chart is shown in Fig. 8, which shows the Genetic Algorithm scores achieved by each trial.

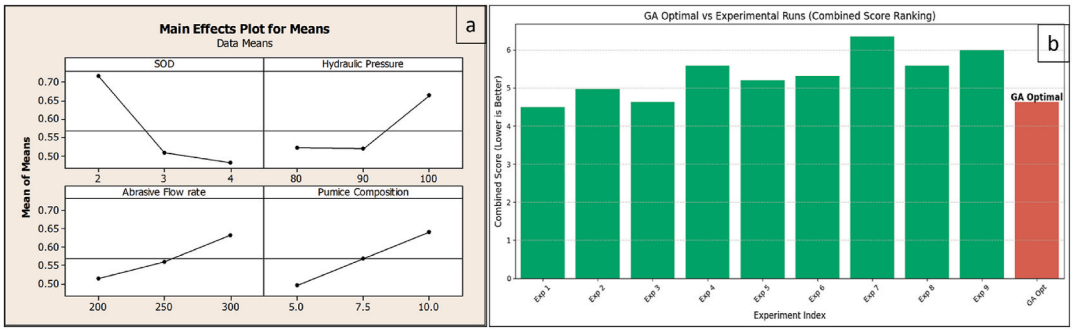

Fig. 8. Optimal parameters suggested by (a) GRA, (b) GA.

Table 5
ANOVA suggesting contribution ranking.

Source	DF	SeqSS	AdjMS	F	P	Contribution
Standoff distance	2	0.06840	0.03420	12.99	0.000	14.07 %
Hydraulic Pressure	2	0.00643	0.00322	1.22	0.319	1.32 %
Abrasive Flow rate	2	0.16518	0.08259	31.31	0.000	33.99 %
Pumice composition Composition	2	0.19854	0.09927	37.63	0.000	40.85 %
Residual Error	18	0.04749	0.00264			9.77 %
Total	26	0.48604				

5. Results and discussion

5.1. Ranking significance of the parameters

Usually, optimising the process which involves more variables is quite difficult. Hence, it is the right methodology to mitigate one or two variables which dominantly contribute to the overall performance of the responses. The two different techniques of ML algorithms, along with the conventional GRA, invariably indicate that the pumice composition influences the machining damages heavily. The ANOVA results obtained from the GRA and shown in Table 5 affirm the higher contribution of pumice composition in the sandwich core to deplete the machining damages, followed by the machining parameter, abrasive flow rate. The same result has been endorsed by the ML algorithms, the linear regression and SHAP through its T-values and SHAP values, respectively. From the analysis of both statistical and soft computing, the hydraulic pressure is considered to be the least significant on the machining damages. The research outcomes preach that the machining damages delamination, kerf width, kerf length and surface roughness can be drastically minimized by controlling pumice composition and abrasive flow rate. The attainment of R^2 and adjR^2 values of more than 90 % indicates that the implemented statistical GRA model is realistic and accurate [37].

5.2. Ideal parameter and pumice composition

The ideal parameter set and pumice composition play an instrumental role in minimizing the machining damage to ensure the machining quality. The prediction of the level of optimal parameters and pumice content by the statistical method GRA and soft computing method GA invariably manifests experiment trial No.3 as the optimal set of parameters and pumice composition. The level of the AWJM parameters and pumice composition is 100 (MPa) of hydraulic pressure, 300 (g/min) of abrasive flow rate, 2 mm of standoff distance, and 10 % of pumice particles. As depicted in Fig. 8 (a), The means secured by the individual variable in experiment trial No.3 are higher than the rest of the experiments, corroborating the optimal nature of the variable in minimizing the damages. Similarly, the overall scores achieved by the GA for the idealness closely match the individual score of the experiment No.3, as shown in Fig. 8 (b).

It can be comprehended from the observation table shown in Table 3 that the machining damages are significantly lesser, whereas, the higher damages are observed from experiment trial No.9, which comprises 4 mm of SOD, 100 bar of hydraulic pressure, 200 g/min of abrasive flow rate and 5 % of pumice composition. Hence, experiments No.3 & 9 are considered to be the best and worst experiments for further discussion on individual effects.

5.3. Effect of parameters on the machining damages

5.3.1. Pumice composition

Both statistical and ML-based predictions invariably acknowledge the higher involvement of pumice composition in downsizing the machining damages. The prediction of the ideal set of parameters reveals a higher percentage of pumice particles inside the core, ensuring the machining quality. Many research reports explored that the intense bonding of the core and cover sheets is dictated by the coarser nature of the particles [38]. The pumice particles used in the study are coarser in surface nature and accelerate the interfacial bonding. Hence the increased interfacial bonding supplemented by the higher content of coarser pumice particles paves the way to retard the delamination as depicted in Fig. 9 (a). Similarly, the lesser content of pumice particles involved in the fabrication of the wt.% 5 specimen exposes an inferior interfacial bonding as illustrated in Fig. 9 (b) It doesn't mean that the mere increased content of pumice particles retards the damage effect rather, the increased interfacial bonding and the subsequent structural integrity are the driving factors to exhaust the damages. Therefore, one of the machining damages is delamination, which is recorded as low for the higher content of the pumice variant. It is well distinguished between the best and worst experiments driven by higher and lower pumice contents, respectively, wherein the higher and lower delamination is observed for the worst and best experiments, shown in Fig. 10 (a) and (b), respectively. The delamination damage is significantly caused by the insufficient interfacial bonding between the core and cover sheets. It is well understood from the micrographs that the higher pumice content acknowledges the strong interfacial bonding, hence the minimal delamination is recorded owing to the more particles with more pronounced surface roughness. Similarly, the lesser pumice content yields poorer interfacial bonding and, in turn, more pronounced delamination is observed. The quantitative comparison between the delamination of wt.% 15 and wt.% 5 pumice loaded specimens manifests that nearly 28 % of delamination damage reduction is recorded for the wt.% pumice sandwich panel in comparison with the wt.% 5 pumice loaded sandwich composite. In contrast to the present finding, a higher

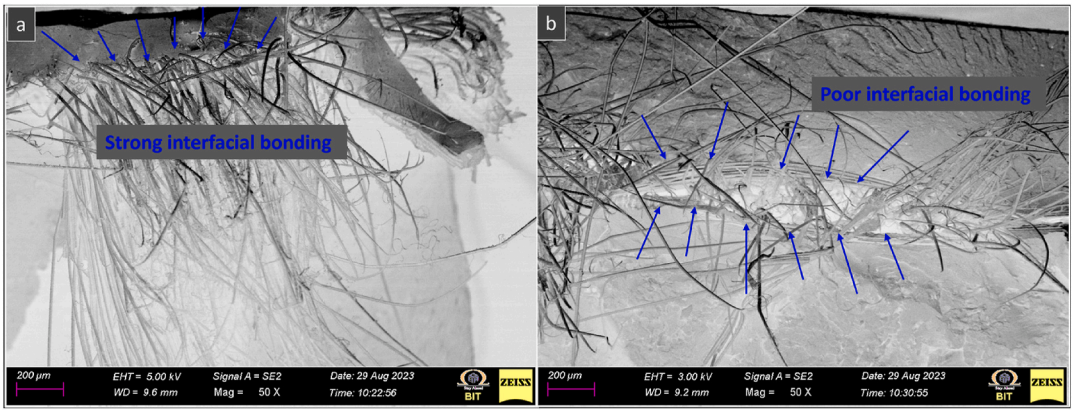

Fig. 9. Micrographs depicting the interfacial bonding (a) Higher pumice content (b) Lower pumice content.

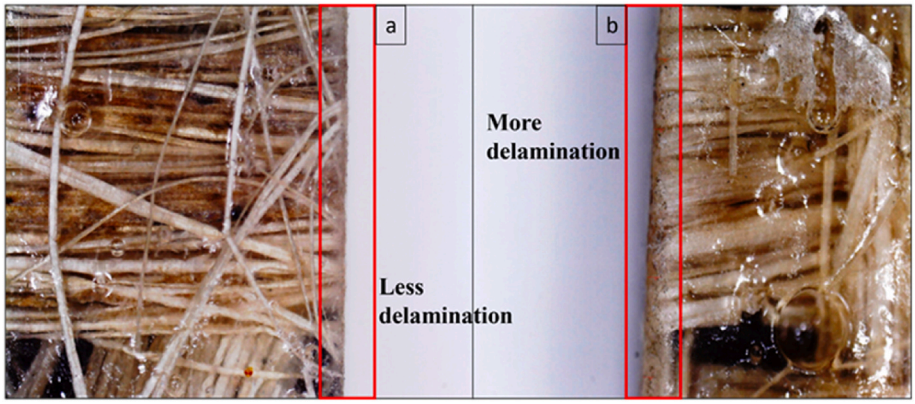

Fig. 10. Delamination results (a) Best experiment (Trial No.3) (b) Worst experiment (Trial No.9).

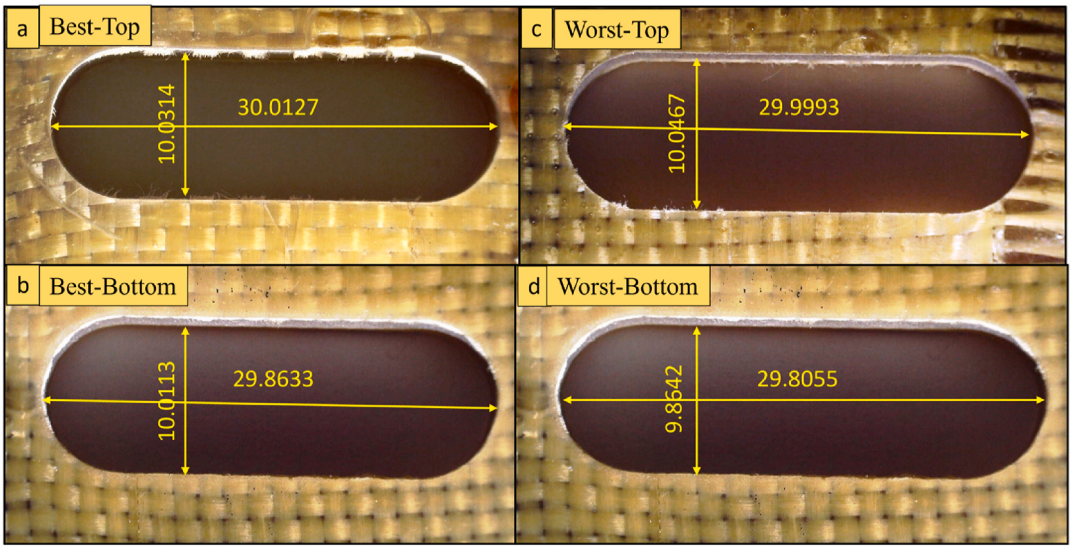

Fig. 11. Kerf damage measurement (a) Worst experiment-top (b) Worst experiment-bottom (c) Best experiment-top (d) Best experiment-bottom.

delamination was reported on the exit side of the abrasive jet than on the entrance side, while the researchers investigated the machining damage on carbon fibre and E-glass fibre woven epoxy composite laminates. The magnitude of the delamination has been reduced by multiple folds in the present study due to the addition of pumice particles. Interestingly, there is no huge delamination difference between the entry and exit of the abrasive jet, as the previous report. The lack of sufficient interfacial bonding between the epoxy and the hybrid carbon-glass fibre owing to the absence of filler particles in the epoxy matrix is concluded as the potential reason for the higher delamination recorded in the previous study.

Usually, kerf taper is induced for two reasons: first, the loss of kinetic energy of the abrasive jet between the top and bottom and second, the jet divergence phenomenon occurring at the bottom of the material. The maximum kinetic energy absorbed at the top layer causes the wider cut, and the minimum kinetic energy causes the narrow cut [39]. This difference in the width of the cut is treated as kerf damage. However, the increased pumice content in the core ensures higher structural integrity due to its improved interfacial bonding, wherein the widening of the cut is greatly controlled by the interaction of higher kinetic energy. It is the physical nature of the abrasive jet to lose its kinetic energy when it interacts with the bottom layer. In technical the structural integrity of the sandwich panel, supplemented by the strong interfacial bonding, facilitates the cutting forces to be distributed uniformly. It can be comprehended that the higher level of interactions of the pumice particles with the Kevlar mat and matrix material, offered by the coarser nature of the particles, help to distribute the cutting force uniformly, hence the minimal kerf damage is recorded. The minimal and maximum kerf damages recorded by the respective samples with higher and lower compositions of pumice particles are depicted in Fig. 11(a)–(b) & **(c)-(d),** respectively.

As far as surface roughness is concerned, the integrity of the material plays a greater role in surface roughness. The higher pumice content intensifies the interfacial bonding between the core and cover sheets, hence, the response of the material against the accelerated abrasive particles is uniform, thereby streamlining the surface roughness. In contrast, the lack of interfacial bonding induced by the lesser content of pumice particles dents the structural integrity of the material, wherein the response of the core and cover sheets against the accelerated abrasive particles is discrete, thereby increasing surface roughness [40]. The quantitative comparison between the surface roughness of wt.% 15 and wt.% 5 pumice loaded specimens manifests that nearly 53.21 % of surface roughness damage reduction is recorded for the wt.% pumice sandwich panel in comparison with the wt.% 5 pumice loaded sandwich composite. However, the higher level of surface roughness between 4.77 and 6.96 μm was reported by the researchers [41] while they experimented with the surface quality of carbon fibre reinforced polymer composite (CFRP) during machining at AWJM. In contrast, the present research involving thermosetting epoxy experiences the surface roughness range of 2.21–4.12 μm, which is 68.93 % of the reduced surface

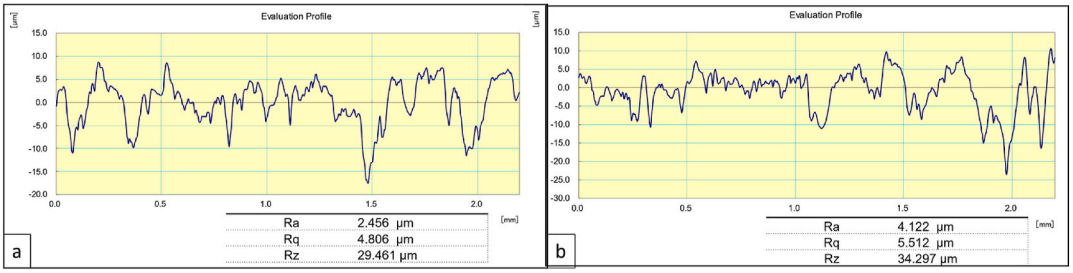

Fig. 12. Surface roughness observation (a) Best experiment (b) Worst experiment.

defects of the previous research study. However, the nature of the material also impacts the surface quality since the previous author claimed that the matrix was thermoplastic polyurethane with a low melting point of 145 °C, hence the poor surface roughness recorded. Interestingly, the minimal surface roughness of 2.45 µm was observed by the researchers [42] while they machined the same CRFP made with thermoplastic polyamide 66, with the melting temperature of 260 °C. It is comprehended from this comparison that the strength of the material influences the surface quality in addition to the AWJM parameters, during machining at AWJM.

The hybrid statistical and soft computing models acknowledge the best and worst experiments, whose minimal and maximum surface roughness are illustrated in Fig. 12 (a) & **(b),** respectively.

5.3.2. Effect of abrasive flow rate

The higher level of abrasive flow rate regulates the kerf taper to be minimal since the loss of kinetic energy at the bottom in comparison to the top layer is compromised with the higher volume of abrasive flow. Usually, the divergence of the abrasive jet with lesser kinetic energy dilutes the cutting ability; hence, the narrow cut is reported [43]. However, the diverged jet enriched with more abrasive particles at a higher abrasive flow rate, which minimizes narrow cuts and kerf taper, is witnessed. The effect of delamination is significantly reduced with a higher abrasive flow rate since it provides a higher cutting force. The higher cutting force prompts to impedes the micro level of lateral movement of coversheets, thereby resulting in less delamination being observed [44]. Furthermore, the surface roughness is also fine-tuned with the uniform cutting nature of the streamline jet enriched with a higher number of abrasive particles. The ideal experiment pointed out from the analysis, experiences lesser machining damages, including kerf taper, delamination and surface roughness, is driven by the higher flow rate of 300 gm/min abrasive particles.

5.3.3. Standoff distance

The increased standoff distance causes a diverging jet and irregular contact of abrasive particles, allowing the cut to expand and hence cause additional kerf damage. In contrast, a small standoff distance provides a focused beam of abrasive jet that supports the narrow cut, minimizing kerf damage [45]. The diverged jet caused by the increased standoff distance enables abrasive particles to embed into the cover sheet by escaping from the plane's stream [46]. This condition of blocked abrasive particles contributes to delamination damage. However, the narrow standoff distance streamlines the flow of abrasive particles, preventing the clogging effect. The reduced standoff distance improves surface roughness by delivering abrasive particles in a targeted manner, contributing to the uniform erosion effect. The ideal parameter dictated by the modelling is a low standoff distance of 2 mm. In contrast, the higher standoff distance of 4 mm linked with subpar testing confirms the history of increased machining damage.

6. Conclusions

The common issue of machining difficulty associated with higher machining damages for the novel Kevlar-pumice sandwich polymer composite is addressed by implementing a hybrid statistical and soft computing approach. There are several constructive conclusions delivered from the study. The fabricated composite sandwich panels are machined through AWJM with the design of L9 orthogonal array. The experimental results analysed through statistical GRA and ML based on Linear regression and SHAP algorithms invariably reveal that experiment No.3 is the optimal run to yield minimal machining damages. The ANOVA and GA analyses highlight the higher contribution of pumice particle content in the core to influence the listed machining damages, significantly. However, the machining parameters, abrasive flow rate and standoff distance play an influential role at subsequent stages. A 90 % above R^2, adjR^2 values in GRA and 1.65 %, 25.41 % and 40.71 % fall in machining damages endorse the accuracy and genuineness of the implemented models. Further, the outcome of the study to deplete the machining damages would benefit the composite manufacturing industries to march towards the modern quality indices and lean manufacturing implementation. The proposed Kevlar-pumice sandwich panel can be utilized in constructional, structural applications like machine housing, furniture, interior partitioners, door panels, lightweight roofings, and impact-resistant panels for lightweight ballistic applications.

Data and code availability

The data involved in the findings of the result will be shared by the corresponding author based on reasonable request.

Declaration of competing interest

The authors declare that they have no known competing financial interests or personal relationships that could have appeared to influence the work reported in this paper.

Acknowledgement

This work was funded by the European Union under the REFRESH-Research Excellence For REgion Sustainability and High-tech Industries project number CZ.10.03.01/00/22_003/0000048 via the Operational Programme Just Transition. The authors extend their appreciation to the Deanship of Research and Graduate Studies at King Khalid University, Kingdom of Saudi Arabia for funding this work through the Large Research Project under the grant number RGP2/143/46. The authors thank the management of Alliance University, Bengaluru for their extended support in demonstrating the research work in successful manner.

References

[1] Hsissou R, et al. Polymer composite materials: a comprehensive review. Compos Struct 2021;262:113640.
[2] Ramalingam K, et al. Novel cellulosic natural fibers from Abelmoschus ficulneus weed: extraction and characterization for potential application in polymer composites. J Polym Environ 2023;31(4):1323–34.

[3] Nurazzi N, et al. A review on mechanical performance of hybrid natural fiber polymer composites for structural applications. Polymers (Basel) 2021;13(13):2170.
[4] Ramakrishna S, et al. Biomedical applications of polymer-composite materials: a review. Compos Sci Technol 2001;61(9):1189–224.
[5] Rajak DK, Wagh PH, Linul E. A review on synthetic fibers for polymer matrix composites: performance, failure modes and applications. Materials (Basel) 2022;15(14):4790.
[6] Rajak DK, et al. Fiber-reinforced polymer composites: manufacturing, properties, and applications. Polymers (Basel) 2019;11(10):1667.
[7] Koniuszewska AG, Kaczmar JW. Application of polymer based composite materials in transportation. Prog Rubber Plast Recycl Technol 2016;32(1):1–24.
[8] Rubino F, et al. Marine application of fiber reinforced composites: a review. J Mar Sci Eng 2020;8(1):26.
[9] Rupal A, et al. Utilization of polymer composite for development of sustainable construction material. Advances in Materials Science and Engineering, 2022 2022;(1):1240738.
[10] Zhao X, et al. Preparation of carbon fibre-reinforced composite panels from epoxy resin matrix of nano lignin polyol particles. J Clean Prod 2023;428:139170.
[11] Borrego L, et al. Fatigue behaviour of glass fibre reinforced epoxy composites enhanced with nanoparticles. Compos B Eng 2014;62:65–72.
[12] Tang Y, et al. Interlaminar fracture toughness and CAI strength of fibre-reinforced composites with nanoparticles–A review. Compos Sci Technol 2013;86:26–37.
[13] Chenrayan V, et al. Flexural integrity of the Kevlar fabric-crumb rubber reinforced sandwich composite: experimental assessment supported by analytical and numerical approaches. J Mater Res Technol 2025.
[14] Bozkurt I. Effect of geometric configurations and curvature angle of corrugated sandwich structures on impact behavior. Polym Compos 2025;46(2):1662–85.
[15] Kumar D, Singh K. An approach towards damage free machining of CFRP and GFRP composite material: a review. Adv Compos Mater 2015;24(sup1):49–63.
[16] Alarifi IM. A review on factors affecting machinability and properties of fiber-reinforced polymer composites. J Nat Fibers 2023;20(1):2154304.
[17] Mm IW, et al. Kerf taper and delamination damage minimization of FRP hybrid composites under abrasive water-jet machining. Int J Adv Des Manuf Technol 2018;94(5):1727–44.
[18] Alqarni AS. A comprehensive review on properties of sustainable concrete using volcanic pumice powder ash as a supplementary cementitious material. Constr Build Mater 2022;323:126533.
[19] Nagarajan B, et al. Tensile, flexural, and fatigue responses of lightweight pumice-reinforced magnesium composite: experimentation followed by an analytical modeling. J Eng Mater Technol 2025;147(3).
[20] Madhu S, Balasubramanian M. Challenges in abrasive jet machining of fiber-reinforced polymeric composites–a review. World J Eng 2021;18(2):251–68.
[21] Chenrayan V, et al. An experimental and empirical assessment of machining damage of hybrid glass-carbon FRP composite during abrasive water jet machining. J Mater Res Technol 2022;19:1148–61.
[22] Dahiya AK, Bhuyan BK, Kumar S. Optimization of process parameters for surface roughness of GFRP with AWJ machining using Taguchi and GRA methods. Int. J. Mod. Manuf. Technol. 2021;13(2):2021.
[23] Brn M, et al. Study on machining quality in abrasive water jet machining of jute-polymer composite and optimization of process parameters through grey relational analysis. Journal of Composites Science 2024;8(1):20.
[24] Jagadish S Bhowmik, Ray A. Prediction and optimization of process parameters of green composites in AWJM process using response surface methodology. Int J Adv Des Manuf Technol 2016;87:1359–70.
[25] Tripathi DR, et al. Experimental investigation and optimization of abrasive waterjet machining parameters for GFRP composites using metaphor-less algorithms. Mater Manuf Process 2021;36(7):803–13.
[26] Ziyad F, et al. Multi-objective optimization of machining parameters of mild steel AISI 1018 under compressed air-assisted cooling by using genetic algorithm. Int J Interact Des Manuf 2024:1–21.
[27] Kumar KN, Babu PD. Improving the machining performance of polymer hybrid composite by abrasive water jet machining for precise machining. Arabian J Sci Eng 2024;49(11):15347–66.
[28] Tanrıverdi S, Aydın L. Optimization of process parameters for green composites in abrasive water jet machining process using neuro-regression analysis. Journal of Artificial Intelligence and Data Science 2021;1(1):71–9.
[29] Vijayananth K, et al. An integrated CRITIC-COPRAS approach for multi-response optimization on AWJM of hybrid filler–reinforced polymer composite and its surface integrity. Int J Adv Des Manuf Technol 2024;131(9):4965–80.
[30] Chenrayan V, et al. Leverage of aluminium oxynitride on the impact resistance of Kevlar-impregnated epoxy composites: experimental and numerical evaluation under low-velocity impact. Polym Compos 2024;45(18):17061–74.
[31] Dhakal HN, et al. Abrasive water jet drilling of advanced sustainable bio-fibre-reinforced polymer/hybrid composites: a comprehensive analysis of machining-induced damage responses. Int J Adv Des Manuf Technol 2018;99:2833–47.
[32] Shetty R, Hegde A. Taguchi based fuzzy logic model for optimisation and prediction of surface roughness during AWJM of DRCUFP composites. Manuf Rev 2022;9:2.
[33] Kalirasu S, et al. AWJM Performance of jute/polyester composite using MOORA and analytical models. Mater Manuf Process 2017;32(15):1730–9.
[34] Chenrayan V, et al. Effect of powder composition, PTAW parameters on dilution, microstructure and hardness of Ni–Cr–Si–B alloy deposition: experimental investigation and prediction using machine learning technique. Heliyon 2024;10(16):e36087.
[35] Periyappillai G, Subbarayan S, Sengottaiyan S. Advanced ensemble machine learning prediction to enhance the accuracy of abrasive waterjet machining for biocomposites. Mater Chem Phys 2025;333:130175.
[36] Phani K, et al. Experimental investigation and optimization of process parameter of abrasive water jet machining (AWJM) on D2 steel. India: New Delhi, India: SAGE Publications Sage; 2025, 25165984241280845.
[37] Faraway JJ. Practical regression and ANOVA using R, vol 168. of Bath Bath: University; 2002.
[38] Van Dam J, et al. Effect of surface roughness and chemistry on the adhesion and durability of a steel-epoxy adhesive interface. Int J Adhesion Adhes 2020;96:102450.
[39] Anu Kuttan A, Rajesh R, Dev Anand M. Abrasive water jet machining techniques and parameters: a state of the art, open issue challenges and research directions. J Braz Soc Mech Sci Eng 2021;43:1–14.
[40] Kumaran ST, et al. Prediction of surface roughness in abrasive water jet machining of CFRP composites using regression analysis. J Alloys Compd 2017;724:1037–45.
[41] Bañon F, et al. Study of the surface quality of carbon fiber–reinforced thermoplastic matrix composite (CFRTP) machined by abrasive water jet (AWJM). Int J Adv Des Manuf Technol 2020;107:3299–313.
[42] Kakinuma Y, et al. Ultrafast feed drilling of carbon fiber-reinforced thermoplastics. Proced CIRP 2015;35:91–5.
[43] de Abreu e Lima CE, et al. Study of influence of traverse speed and abrasive mass flowrate in abrasive water jet machining of gemstones. Int J Adv Des Manuf Technol 2016;83:77–87.
[44] Natarajan Y, et al. Abrasive Water Jet Machining process: a state of art of review. J Manuf Process 2020;49:271–322.
[45] Abouzaid A, Mousa S, Ibrahim AMM. Effect of standoff distance and traverse speed on the cutting quality during the abrasive water jet machining (AWJM) of brass. Mach Sci Technol 2024;28(3):392–414.
[46] Mohamad W, et al. Effect of standoff distance on the kerf characteristic during abrasive water jet machining. Results Eng 2020;6:100101.